

RATES OF ADSORPTION OF CO₂ ON HYDROTALCITE

NADIA BINTI ISA

**UNIVERSITI SAINS MALAYSIA
2011**

RATES OF ADSORPTION OF CO₂ ON HYDROTALCITE

by

NADIA BINTI ISA

**Thesis submitted in fulfilment of the
requirements for the degree
of Master of Science**

FEBRUARY 2011

ACKNOWLEDGEMENTS

Firstly, I would like to express my genuine appreciation to my supervisor, Assoc. Prof. Dr. W.J.N. Fernando for his wonderful supervision and the enormous time and effort he spent for guiding and assisting me throughout the accomplishment of my master program. His advices and guidance has always enlightened my thinking and ideas in my research work. Also, I would like to extend my gratitude to my co-supervisor Prof. Dr. Abdul Latif Ahmad for his brilliant comments and encouragement. I was honoured to have the opportunity to work under the supervision of both of you.

I would like to thank the Dean of School of Chemical Engineering, Universiti Sains Malaysia (USM), Prof. Dr. Azlina Harun@Kamaruddin and the Deputy Deans, Assoc. Prof. Dr. Lee Keat Teong and Assoc. Prof. Dr. Mohamad Zailani bin Abu Bakar for their continuous support and help rendered throughout my studies. I am also indebted to School of Chemical Science, School of Physics and School of Material and Mineral Engineering in USM for the TGA, SEM and XRD analysis.

My sincere thanks to all the respective lecturers, staff and technicians of School of Chemical Engineering for their co-operation and supports. Thousand thanks to Mr. Syamsul Hidayat Shaharan, Mr. Mohd Faiza Ismail and Mr. Muhd Arif Mat Husin for their valuable and kind help in the laboratory works. Thanks also to my colleagues who always having discussion with me whenever I am confronted

with any difficulties. Also to those who are directly and indirectly involved in this research, your contributions shall not be forgotten.

My deepest gratitude goes to my family who always being understanding and supportive throughout my postgraduate life. With their endless love and supports, I was able to concentrate in my research work without fears and worries.

Lastly, I would like to express my acknowledgement to USM. This research study might not be able to carry out without the financial supports from Exxon Mobil Grant for Research/ Higher Education, USM Fundamental Research Fund Scheme , RU Grant and the Fellowship from the Ministry of Science, Technology and Innovation (MOSTI).

Nadia Isa

Engineering Campus USM, 2011

TABLE OF CONTENTS

	Page
AKNOWLEDGEMENTS	ii
TABLE OF CONTENTS	iv
LIST OF TABLES	ix
LIST OF FIGURES	x
LIST OF PLATES	xv
LIST OF NOMENCLATURE	xvi
LIST OF ABBREVIATION	xx
LIST OF APPENDICES	xxii
ABSTRAK	xxiii
ABSTRACT	xxv

CHAPTER ONE : INTRODUCTION

1.1 Carbon Dioxide – Need for separation	1
1.2 Methods of separation of carbon dioxide	4
1.2.1 Separation of CO ₂ by adsorption onto hydrotalcite	4
1.2.2 Separation of CO ₂ by membranes of hydrotalcite	7
1.2.3 Other methods	10
1.2.4 Gas diffusion	13
1.3 Problem Statement	14
1.4 Objectives	15
1.5 Scope of Study	16
1.6 Organization of the Thesis	17

CHAPTER TWO : LITERATURE REVIEW

2.1 Hydrotalcite	19
2.1.1 General description	19
2.1.2 Hydrotalcites: Synthesis and characterization	22
2.1.2 (a) Hydrotalcites from co-precipitation method	23

2.1.2 (b) Hydrotalcites from hydrothermal treatment method	25
2.1.2 (c) Hydrotalcites from urea hydrolysis	27
2.1.2 (d) Hydrotalcite from sol gel method	28
2.2 Separation of Carbon dioxide using Hydrotalcite	31
2.2.1 Studies on adsorption of CO ₂ on hydrotalcite	33
2.2.2 Separation of CO ₂ using membrane coats of hydrotalcite	41
2.3 Theoretical studies on rates of adsorption of CO ₂	45
2.4 Design of Experiment (DoE) and ANOVA	55
2.4.1 Response Surface Methodology (RSM)	56
2.4.2 Central Composite Design (CCD)	59
2.5 Summary	60

CHAPTER THREE : MATERIALS AND METHODS

3.1 Chemicals	61
3.2 Equipment	62
3.2.1 Equipment used for preparation of samples	62
3.2.2 Measuring equipment	63
3.2.2 (a) Brunauer Emmett and Teller (BET) analyzer	63
3.2.2 (b) X-ray diffraction (XRD) analyzer	63
3.2.2 (c) Scanning electron microscope (SEM) analyzer	64
3.2.2 (d) Thermal gravimetric (TGA) analyzer	64
3.2.3 Experimental rig	64
3.2.3 (a) Batch reactor	64
3.2.3 (b) Tubular furnace	66
3.2.3 (c) The set up	67
3.3 Preliminary studies and experimental procedures	68
3.3.1 Preparation of synthetic hydrotalcite	70
3.3.2 Selection of source of hydrotalcite for samples in experimentation	70
3.3.3 Preparation of sol gel membrane	71

3.3.3 (a) Binder	71
3.3.3 (b) Preparation of sol gel	72
3.3.4 Preparation of pellets	72
3.3.5 Coating of pellets	73
3.3.6 Batch adsorption experiments	73
3.3.6 (a) Initial leak tests	73
3.3.6 (b) Determination of rates of adsorption	73
3.4 Rate determining experiments	75
3.4.1 Experiments with hydrotalcite powder	75
3.4.2 Experiments with hydrotalcite pellets	75
3.4.2 (a) Temperature of reaction	76
3.4.2 (b) Diameter of pellets	76
3.4.2 (c) Number of coatings on pellet	77
3.5 Theoretical studies	78
3.5.1 Pseudo first order model	79
3.5.2 Pseudo second order model	80
3.5.3 Langmuir kinetic model	81
3.5.4 External diffusion control model	81
3.5.5 Internal diffusion control model	82
3.5.6 Dual site Langmuir (DSL) model	83
3.5.7 Extended model of Langmuir with surface modification	84
3.6 Selection of appropriate model	86
3.7 ANOVA analysis	86
3.8 Optimization	87

CHAPTER FOUR : RESULTS AND DISCUSSION

4.1 Preliminary studies: Selection of sources of hydrotalcite	88
4.2 Preliminary studies: Characterization of hydrotalcite	91
4.2.1 Thermo gravimetric (TGA) analysis	92
4.2.2 X-ray diffraction (XRD) analysis	93
4.2.3 Scanning electron microscope (SEM) analysis	96
4.2.4 Analysis of adsorption area of hydrotalcite towards CO ₂	99

4.2.5	General observations	101
4.3	Rates of adsorption	101
4.3.1	Rates of adsorption of CO ₂ on hydrotalcite powder	102
4.3.2	Rates of adsorption of CO ₂ on hydrotalcite pellets	103
4.3.2 (a)	Variation of rates of adsorption of CO ₂ with different number of coating	105
4.3.2 (b)	Variation of rates of adsorption of CO ₂ with different diameter of pellets	109
4.4	Theoretical analysis of adsorption of CO ₂ on hydrotalcite	111
4.4.1	Investigation of pseudo first order model	111
4.4.2	Investigation of pseudo second order model	112
4.4.3	Investigation of Langmuir kinetic model	114
4.4.4	Investigation of diffusion models	115
4.4.4 (a)	Investigation of applicability of external diffusion control model	115
4.4.4 (b)	Investigation of effects of internal diffusion control model	116
4.4.5	Dual site Langmuir (DSL) model	116
4.4.6	Extended Langmuir model with surface modifications	117
4.5	Statistical analysis of parameters of the extended model of Langmuir (with surface modifications)	122
4.5.1	Parameter: K_I	122
4.5.2	Parameter: Initial forward rate constant (K_2)	126
4.5.3	Parameter: Rate constant (k_{-1})	129
4.6	Re-validation of the extended Langmuir model	133
4.7	Summary	133
 CHAPTER FIVE : CONCLUSION		
5.1	Conclusions	134
5.2	Recommendations	136
 REFERENCES		137

APPENDICES	151
APPENDIX A	151
APPENDIX B	159
LIST OF PUBLICATIONS AND SEMINARS	160

LIST OF TABLES

		Page
Table 3.1	List of chemicals used	61
Table 3.2	Details of equipment used for preparation of samples	62
Table 3.3	Experimental range and levels of independent variables	77
Table 3.4	Central composite design layout	78
Table 4.1	Physical properties of hydrotalcite	89
Table 4.2	Adsorption capacity of hydrotalcite	100
Table 4.3	Values of parameters of K_1 , K_2 , k_{-1} and correlation coefficient (R^2) for hydrotalcite powder	120
Table 4.4	Values of parameters of K_1 , K_2 , k_{-1} and correlation coefficient (R^2) for DoE runs of hydrotalcite pellets	121
Table 4.5	Analysis of variance for the 2FI model for parameter of (K_1) ($\text{min}^{-1} \cdot \text{bar}^{-1}$)	123
Table 4.6	Analysis of variance for the 2FI model of the initial forward rate constant (K_2) ($\text{g}_{\text{CO}_2} \cdot \text{g}_{\text{HT}}^{-1} \cdot \text{min}^{-1} \cdot \text{bar}^{-1}$)	127
Table 4.7	Analysis of variance for the quadratic model for the rate constant (k_{-1}) (min^{-1})	130

LIST OF FIGURES

		Page
Figure 1.1	Comparison between the brucite and the hydrotalcite structures (Serwicka and Bahranowski, 2004).	6
Figure 2.1	3-D structure model for hydrotalcite (Tsunashima and Toshiyuki, 1999).	20
Figure 2.2	2-D structure models for hydrotalcite (Yong and Rodrigues, 2002).	20
Figure 2.3	Schematic diagram showing the formation of membrane film by dip-coating with sol gel mixture (Brinker <i>et al.</i> , 1993).	30
Figure 2.4	The IUPAC classification of adsorption isotherms for gas-solid equilibria (Donohue and Aranovich, 1998)	34
Figure 2.5	N ₂ adsorption/desorption isotherms at 77K of the as-synthesized and decomposed samples with or without steam (Abello and Perez-Ramirez, 2006).	35
Figure 2.6	Adsorption isotherms for CO ₂ adsorption on hydrotalcite at 200°C after preheating in vacuum at 200°C and 400°C (Hutson <i>et al.</i> , 2004).	36
Figure 2.7	CO ₂ sorption data in fixed bed reactor and simulated breakthrough curves of some oxides (Wang <i>et al.</i> , 2008).	37
Figure 2.8	The initial rate of adsorption versus temperature for CuAl-2.0 adsorbent (Ye Lwin and Abdullah, 2009).	38
Figure 2.9	Adsorption isotherms of CO ₂ on hydrotalcite samples at 20°C, 200°C and 300°C for (a) EXM696 and (b) EXM911 (Yong <i>et al.</i> , 2001).	39
Figure 2.10	Sorption equilibrium isotherms of CO ₂ on hydrotalcite modified with potassium at 579, 676 and 783K (Oliveira <i>et al.</i> , 2008). Note: Solid line, bi-Langmuir model; dashed line, physical adsorption contribution to the model; dotted line, chemical reaction contribution to the model	40

Figure 2.11	The sorption site of two distinct adsorption sites (Krishna <i>et al.</i> , 1999).	54
Figure 2.12	Central composite design model (Cho and Zoh, 2006)	60
Figure 3.1	Schematic diagram of batch reactor	66
Figure 3.2	Schematic diagram of fabricated experimental rig	67
Figure 3.3	Flowchart of research methodology	69
Figure 3.4	Flowchart for Mathworks MATLAB & Simulink (Version R2009a) programming	87
Figure 4.1	XRD pattern of synthetically prepared of a fresh hydrotalcite sample	90
Figure 4.2	XRD pattern of a commercially available of fresh hydrotalcite sample	90
Figure 4.3	Thermo gravimetric analysis of fresh commercial hydrotalcite	93
Figure 4.4	XRD pattern of hydrotalcite (Tomita-AD500) after subsequent heat treatment at 300°C	94
Figure 4.5	XRD pattern of hydrotalcite (Tomita-AD500) after subsequent heat treatment at 450°C	95
Figure 4.6	XRD pattern of hydrotalcite (Tomita-AD500) after subsequent heat treatment at 550°C	95
Figure 4.7	XRD pattern of hydrotalcite (Tomita-AD500) after subsequent heat treatment at 700°C	96
Figure 4.8	SEM image of commercial hydrotalcite prior to reaction at 32°C	97
Figure 4.9	SEM image of commercial hydrotalcite after reaction with CO ₂ at 32°C	98
Figure 4.10	SEM image of commercial hydrotalcite prior to reaction at 450°C	98
Figure 4.11	SEM image of commercial hydrotalcite after reaction with CO ₂ and heat treatment at 450°C	98
Figure 4.12	SEM image of commercial hydrotalcite prior to reaction at 550°C	99

Figure 4.13	SEM image of commercial hydrotalcite after reaction with CO ₂ and heat treatment at 550°C	99
Figure 4.14	Variation of partial pressure with time for powdered hydrotalcite with different temperatures of reaction	103
Figure 4.15	Plots of adsorption of CO ₂ versus partial pressure for powdered hydrotalcite with different temperatures of reaction	103
Figure 4.16	Variation of partial pressure with time for hydrotalcite pellets of no coating for different temperatures and diameter of pellets	104
Figure 4.17	Variation of partial pressure with time for hydrotalcite pellets of single coating for different temperatures and diameter of pellets	104
Figure 4.18	Variation of partial pressure with time for hydrotalcite pellets of double coatings for different temperatures and diameter of pellets	104
Figure 4.19	Plots of rates of adsorption versus partial pressure of CO ₂ for pelletized hydrotalcite at temperature of reaction of 32°C for 8mm pellets of zero and double coatings	107
Figure 4.20	Plots of rates of adsorption versus partial pressure of CO ₂ for pelletized hydrotalcite at temperature of reaction of 32°C for 20mm pellets of zero and double coatings	107
Figure 4.21	Plots of rates of adsorption versus partial pressure of CO ₂ for pelletized hydrotalcite at temperature of reaction of 300°C for 15mm pellets of zero, single and double coatings	108
Figure 4.22	Plots of rates of adsorption versus partial pressure of CO ₂ for pelletized hydrotalcite at temperature of reaction of 550°C for 8mm pellets of zero and double coatings	108
Figure 4.23	Plots of rates of adsorption versus partial pressure of CO ₂ for pelletized hydrotalcite at temperature of reaction of 550°C for 20mm pellets of zero and double coatings	108
Figure 4.24	Plots of rates of adsorption versus partial pressure of CO ₂ for pelletized hydrotalcite at temperature of reaction of 32°C for 8mm and 20mm pellets of no coating	110
Figure 4.25	Plots of rates of adsorption versus partial pressure of CO ₂ for pelletized hydrotalcite at temperature of reaction of 32°C for 8mm and 20mm pellets of double coatings	110

Figure 4.26	Plots of rates of adsorption versus partial pressure of CO ₂ for pelletized hydrotalcite at temperature of reaction of 300°C for 8mm, 15mm and 20mm pellets of single coating	110
Figure 4.27	Plots of rates of adsorption versus partial pressure of CO ₂ for pelletized hydrotalcite at temperature of reaction of 550°C for 8mm and 20mm pellets of double coatings	111
Figure 4.28	Plot of t/Q_t (min/g _{CO2} /g _{HT}) versus time (min) at various temperatures for hydrotalcite powder	113
Figure 4.29	Plot of t/Q_t (min/g _{CO2} /g _{HT}) versus time (min) at various temperatures for hydrotalcite pellets at diameter of 8mm pellets	113
Figure 4.30	Plot of t/Q_t (min/g _{CO2} /g _{HT}) versus time (min) at various temperatures for hydrotalcite pellets at diameter of 15mm pellets	113
Figure 4.31	Plot of t/Q_t (min/g _{CO2} /g _{HT}) versus time (min) at various temperatures for hydrotalcite pellets at diameter of 20mm pellets	114
Figure 4.32	Plots of extended model of Langmuir at temperature of 32°C for hydrotalcite powders	119
Figure 4.33	Plots of extended model of Langmuir at temperature of 300°C and 550°C for hydrotalcite powders	119
Figure 4.34	Plots of extended model of Langmuir at temperature of 32°C for hydrotalcite pellets	119
Figure 4.35	Plots of extended model of Langmuir at temperature of 300°C for hydrotalcite pellets	120
Figure 4.36	Plots of extended model of Langmuir at temperature of 550°C for hydrotalcite pellets	120
Figure 4.37	Parity plot for the experimental and predicted of K_I (min ⁻¹ .bar ⁻¹) from Equation 4.1(b)	123
Figure 4.38	3D plot of parameter of K_I (min ⁻¹ .bar ⁻¹) versus diameter of pellets (mm) and temperatures of reaction (°C) for without coating pellets	125
Figure 4.39	3D plot of parameter of K_I (min ⁻¹ .bar ⁻¹) versus diameter of pellets (mm) and temperatures of reaction (°C) for single coating pellets	125

Figure 4.40	3D plot of parameter of K_1 ($\text{min}^{-1} \cdot \text{bar}^{-1}$) versus diameter of pellets (mm) and temperatures of reaction ($^{\circ}\text{C}$) for double coatings pellets	125
Figure 4.41	Parity plot for the experimental and predicted K_2 ($\text{g}_{\text{CO}_2} \cdot \text{g}_{\text{HT}}^{-1} \cdot \text{min}^{-1} \cdot \text{bar}^{-1}$) from Equation 4.2(b)	127
Figure 4.42	3D plot of initial forward rate constant (K_2) ($\text{g}_{\text{CO}_2} \cdot \text{g}_{\text{HT}}^{-1} \cdot \text{min}^{-1} \cdot \text{bar}^{-1}$) versus diameter of pellets (mm) and temperatures of reaction ($^{\circ}\text{C}$) for without coating pellets	128
Figure 4.43	3D plot of initial forward rate constant (K_2) ($\text{g}_{\text{CO}_2} \cdot \text{g}_{\text{HT}}^{-1} \cdot \text{min}^{-1} \cdot \text{bar}^{-1}$) versus diameter of pellets (mm) and temperatures of reaction ($^{\circ}\text{C}$) for single coating pellets	128
Figure 4.44	3D plot of initial forward rate constant (K_2) ($\text{g}_{\text{CO}_2} \cdot \text{g}_{\text{HT}}^{-1} \cdot \text{min}^{-1} \cdot \text{bar}^{-1}$) versus diameter of pellets (mm) and temperatures of reaction ($^{\circ}\text{C}$) for double coatings pellets	129
Figure 4.45	Parity plot for the experimental and predicted k_{-1} (min^{-1}) from Equation 4.3(b)	131
Figure 4.46	3D plot of parameter of k_{-1} (min^{-1}) versus diameter of pellets (mm) and temperatures of reaction ($^{\circ}\text{C}$) for without coating pellets	132
Figure 4.47	3D plot of parameter of k_{-1} (min^{-1}) versus diameter of pellets (mm) and temperatures of reaction ($^{\circ}\text{C}$) for single coating pellets	132
Figure 4.48	3D plot of parameter of k_{-1} (min^{-1}) versus diameter of pellets (mm) and temperatures of reaction ($^{\circ}\text{C}$) for with double coatings pellets	132
Figure 4.49	Plot of predicted rates of adsorption versus experimental rates of adsorption for hydrotalcite pellets	133

LIST OF PLATES

		Page
Plate 3.1	Image of fabricated batch reactor	65
Plate 3.2	Image of fabricated experimental rig consisting of tubular furnace, a batch reactor and a controller	68

LIST OF NOMENCLATURE

Symbol	Description	Unit
+1	High level	-
-1	Low level	-
A	Factor code for temperatures of reaction in DoE	-
a_z	External area of granule per unit volume of mixed bed	m^{-1}
B	Factor code for diameter of pellets in DoE	-
b_0	Offset term	-
b_j	Linear effect	-
b_{ij}	First order interaction effect	-
b_{jj}	Squared effect	-
C	Factor code for number of coatings in DoE	-
C	Intercept	-
C_A	Concentration of A in the outlet stream	mol/cm^3
D_o	Maxwell Stefan diffusivity	m^2/s
K_1	$k_1\alpha$	m^2/min
K_2	$k_1\beta$	$g_{CO_2}/g_{HT}/min^2$
K_a, K_d	Temperature dependent constants	-
K_E	Equilibrium adsorption constant for site E	Pa^{-1}
K_F	Equilibrium adsorption constant for site F	Pa^{-1}
K_p	Intraparticle diffusion rate constant	$g_{CO_2}/g_{HT}/min^{0.5}$
k	Rate constant	-
k_1	Pseudo first order rate constant	min^{-1}

k_2	Pseudo second order rate constant	$\text{g}_{\text{HT}}/\text{g}_{\text{CO}_2}/\text{min}$
k_g	External film mass transfer coefficient	m/s
k_p	Solid film mass transfer coefficient	m/s
k_{-1}	Rate constant of desorption	min^{-1}
N_i^{total}	Total molar flux of each component	-
n	Order of adsorption kinetic model	-
P	Total pressure of CO_2 within the reactor	bar
P_0	Initial total pressure of CO_2 within the reactor	bar
p	Partial pressure of CO_2 within the reactor at time t	bar
p_A	Partial pressure of adsorbate A in the gas	bar
p_0	Initial partial pressure of CO_2 within the reactor	bar
p_i	Partial pressures of all components in the mixtures	bar
Q	Volumetric flowrate	cm^3/min
Q	Total CO_2 adsorbed within a time t of the experiment	$\text{g}_{\text{CO}_2}/\text{g}_{\text{HT}}$
Q_e	Amount of CO_2 adsorbed at ultimate adsorption	$\text{g}_{\text{CO}_2}/\text{g}_{\text{HT}}$
Q_∞	Maximum amount of CO_2 that could be adsorbed by the hydrotalcite	$\text{g}_{\text{CO}_2}/\text{g}_{\text{HT}}$
Q_v	Vacant site of adsorption	$\text{g}_{\text{CO}_2}/\text{g}_{\text{HT}}$
Q_s	Saturation capacity of A	g_A/g_B
q	Amount adsorbed of each component	
q_A^{sat}	Amount of CO_2 adsorbed for site E	$\text{g}_{\text{CO}_2}/\text{g}_{\text{HT}}$
q_B^{sat}	Amount of CO_2 adsorbed for site F	$\text{g}_{\text{CO}_2}/\text{g}_{\text{HT}}$
q_e	Adsorption capacity at maximum	-
q_t	Adsorption capacity at time t	-

R	Gas constant	ml.bar.mol ⁻¹ .K ⁻¹
r^*	Equilibrium parameter	dimensionless
T	Temperature within the reactor	K
t	Contact time	minute
V	Total volume of reactor	ml
v	Volume of hydrotalcite within the reactor	ml
W	Sorbent mass	gram
X	Coded value of the i th independent variable	-
X_i	Natural value of the i th independent variable	-
X_i^x	Natural value of the i th independent variable at the centre point	-
Δ_{Xi}	Step change value	-
x	Mole fraction	-
x_i	Test factors	-
Y	Predicted response	-

Greek symbols

Å	Angstrom, 10 ⁻⁸	-
β	Constant in the integration step	-
δ	Thickness of adsorbent layer	m
ϵ	Intergranular void fraction	dimensionless
ϵ_p	Particle porosity	-
κ_0	Initial sorption rate constant	cm ³ /min.g
κ_d	Deactivation rate constant	min ⁻¹
α_1	Constant for site E	-
α_2	Constant for site F	-

α	Proportional constant	-
ρ	Density of adsorbent	kg/m ³
ρ_s	Density of the solid material	-

LIST OF ABBREVIATIONS

Symbol	Description
A^{n-}	Charge compensating the anion
$Al(NO_3)_3 \cdot 9H_2O$	Aluminium nitrate nonahydrate
ANOVA	Analysis of variance
BET	Brunauer Emmett and Tellet
CH ₄	Methane gas
CO ₂	Carbon dioxide gas
$CO_3^{2-}, Cl^-, NO_3^-, SO_4^{2-}$	Anions
$C_{12}H_{27}AlO_3$	Aluminium secondary butoxide
C_2H_5OH	Ethanol
CCD	Central Composite Design
CVD	Chemical vapour disposition
Ca	Calcium
Co	Cobalt
CaCO ₃	Calcium carbonate
Cu	Cuprum
CPO	Catalytic partial oxidation
DoE	Design of experiment
DSL	Dual site Langmuir
H ₂	Hydrogen
H_2O	Deionized water
HCl	Hydrochloric acid
HT	Hydrotalcite

IUPAC	International Union of Pure and Applied Chemists
K_2CO_3	Potassium carbonate
LDH	Double layered hydroxides
$Mg(NO_3)_2 \cdot 6H_2O$	Magnesium nitrate hexahydrate
$Mg_6Al_2(OH)_{16}CO_3 \cdot 4H_2O$	Commercial hydrotalcite (Tomita-AD500)
Mg/Al	Magnesium to aluminium ratio
MgO	Periclase (Magnesium oxide)
N_2	Nitrogen
$NaOH$	Sodium hydroxide
N^{a+}	Sodium ion
OH^-	Hydroxyl ion
PVB	Ployvinyl(butyral-co-vinyl alcohol) covinyl acetate
RSM	Response surface methodology
R^2	Correlation coefficient
SEM	Scanning electron microscope
SR	Steam reforming
TGA	Thermal gravimetric analyser
TSE	Tensile strength effect
V1	Valve one
V2	Valve two
V3	Valve three
V4	Valve four
wt%	Weight percentage

LIST OF APPENDICES

	Pages	
A.1	MATLAB command of pseudo first order model	151
A.2	Pseudo second order model	152
A.3	MATLAB command of Langmuir kinetic model	153
A.4	MATLAB command of external diffusion control model	154
A.5	MATLAB command of internal diffusion control model	155
A.6	MATLAB command of Dual site langmuir (DSL) model	156
A.7	Linear equations of extended model of Langmuir with surface modification based on DoE runs	157
A.8	Particle size analysis	157
B.1	Calculations of estimated monolayer areas of adsorption of CO ₂ per gram of hydrotalcite	159

KADAR PENJERAPAN CO₂ KE ATAS HIDROTALSIT

ABSTRAK

Dewasa ini hidrotalsit telah menarik perhatian di dalam teknologi pemisahan CO₂ kerana kebolehnya untuk menyerap CO₂ dengan kuantiti yang besar berbanding dengan penyerap yang lain. Banyak kajian telah dijalankan untuk menyiasat struktur dan keseimbangan kapasiti penyerapan CO₂ ke atas hidrotalsit dengan suhu. Namun, kajian terhadap kadar penyerapan CO₂ yang merupakan aspek penting di dalam menentukan kebolehjayaan pemisahan CO₂ masih belum dikaji dengan mendalam lagi. Oleh itu, telah menjadi keperluan untuk mengkaji kadar penyerapan CO₂ terhadap hidrotalsit. Walaupun serbuk hidrotalsit telah menunjukkan keupayaan yang bagus dalam pemisahan CO₂, tetapi penyelenggaraan yang kompleks bagi serbuk hidrotalsit skala komersil adalah dijangkakan. Perkara ini boleh diatasi dengan menggunakan pellet sebagai alternatif kepada serbuk. Oleh itu, kajian ini bertujuan untuk mengkaji kadar penyerapan CO₂ ke atas hidrotalsit di dalam bentuk serbuk dan pelet. Ujikaji telah dijalankan untuk menentukan kadar penyerapan CO₂ ke atas hidrotalsit komersil dalam bentuk serbuk dan pelet berdiameter (8mm, 15mm dan 20mm) pada suhu 32°C, 300°C dan 550°C masing-masing. Ujikaji juga dijalankan untuk menentukan kadar penyerapan CO₂ ke atas hidrotalsit dalam bentuk pelet yang disaluti oleh membran hidrotalsit yang disediakan melalui kaedah sol gel. Satu dan dua lapisan salutan ke atas pelet melalui kaedah salutan celup dikaji. Ujikaji ke atas pelet dijalankan berdasarkan Design of Experiments (DoE). Beberapa model teori lazim dikaji untuk menyiasat kinetik penyerapan CO₂ ke atas hidrotalsit. Data-data ujikaji didapati tidak serasi dengan

model-model lazim. Berdasarkan kajian ke atas analisis oleh Mikroskop Elektron Imbasan (SEM), analisis oleh Permeteran Graviti Haba (TGA) dan analisis oleh Belauan Sinar-X (XRD), satu model menggabungkan modifikasi permukaan hidrotalsit dengan kebolehsuran penjerapan CO₂ dirumuskan dan dikaji bagi memadankan model tersebut dengan data-data ujikaji. Parameter-parameter model tersebut dianalisis secara statistik. Data-data ujikaji didapati padan dengan model yang berdasarkan modifikasi permukaan hidrotalsit dengan nilai pekali sekaitan dari 0.904 ke 0.923 untuk hidrotalsit di dalam bentuk serbuk dan dari 0.827 ke 0.961 untuk hidrotalsit di dalam bentuk pelet.

RATES OF ADSORPTION OF CO₂ ON HYDROTALCITE

ABSTRACT

Hydrotalcite has recently attracted the attention in CO₂ removal technology because of its ability to adsorb appreciable amounts of CO₂ compared with many others adsorbents. Many studies have been carried out in order to investigate the structure and equilibrium adsorption capacities of CO₂ hydrotalcite with different temperatures. However, studies on the rates of adsorption of CO₂, which is an important aspect in the determination of the viability of the removal of CO₂ have not been addressed so far. Hence it has become necessary to study the rates of adsorption of CO₂ on hydrotalcite. Even though hydrotalcite powders have shown excellent potential for removal of CO₂, complexities of handling hydrotalcite powders in commercial scale can be expected. This could be overcome by the use of pellets of hydrotalcite as an alternative to powders. Therefore, this study is aimed for studying the rates of adsorption of CO₂ on hydrotalcite powders as well as pellets. Experiments were conducted to determine the adsorption rates of CO₂ on commercial hydrotalcite powder and pellets of three different diameters (8mm, 15mm and 20mm) at the temperatures of 32°C, 300°C and 550°C respectively. Experiments were also conducted to determine the rates of adsorption of CO₂ on pellets coated with hydrotalcite membrane prepared by sol gel method. Single and double coatings on pellets by dip-coating method were examined. The experiments for pellets were conducted based on Design of Experiments (DoE). Several conventional theoretical

models were examined in order to investigate the kinetics of adsorption of CO₂ onto hydrotalcite. The experimental data were not compatible with the conventional models. Based on the studies of Scanning Electron Microscope (SEM) analysis, Thermo Gravimetric analysis (TGA) and X-ray Diffraction (XRD) analysis, a model incorporating surface modifications of hydrotalcite with progressive adsorption of CO₂ was formulated and examined for fit with experimental data. The model parameters were statistically analysed. The experimental data was observed to fit the model of surface modifications of hydrotalcite satisfactorily with correlation coefficients ranging from 0.904 to 0.923 for hydrotalcite powder and 0.827 to 0.961 for hydrotalcite pellets.

CHAPTER 1

INTRODUCTION

1.1 Carbon dioxide – Need for separation

The sequestration of carbon dioxide emission is important in the present day context in relation to global warming as well as for better utilization of fuels such as treatment of natural gas, controlling of carbon dioxide (CO₂) emissions from fossil fueled power plants and other industrial gases, the production of hydrogen gas and in the aerospace industry (Ye Lwin and Abdullah, 2009, Belmabkhout *et al.*, 2009).

Natural gas is a gaseous fossil fuel consisting primarily of methane (70% - 90%) but including significant quantities of ethane (5% - 15%), butane (<5%), propane (<5%), carbon dioxide (approximately 5%) and small amounts of nitrogen, helium and hydrogen sulfide (Esteves *et al.*, 2008). CO₂ is an impurity which must often be removed from natural gas streams (Kelman *et al.*, 2007). The calorific value of natural gas is generally low with the existence of CO₂. This leads to the requirements of handling higher volumes of natural gas in applications. As a result, the removal of carbon dioxide from natural gas is important in order to increase the calorific value and transportability of natural gas.

Natural gas also must be pre-processed to meet the pipeline specification of 2% to 5% carbon dioxide (Datta and Sen, 2006) prior to transportation through pipelines. The levels of carbon dioxide need to be reduced in order to avoid the formation of solids in cryogenic units and steel pipe corrosion. Carbon dioxide can

be considered as an inert gas with no heating value, therefore it needs to be removed to low levels before it is distributed to the final users (Tagliabue *et al.*, 2009).

CO₂ emissions for conventional vehicles can be reduced and this is a beneficial effect to reduce global warming (Esteves *et al.*, 2008). As the world widely depends on fossil fuels for its energy requirement needs and as this will continue for the foreseeable future, the development of the technology of CO₂ capture and storage becomes increasingly important. The combustion of fossil fuels such as coal or natural gas releases large volumes of carbon dioxide into the environment and this has become the most serious global environmental problem (Yong *et al.*, 2002). It is forecasted that CO₂ emissions are expected to double by the year 2030 (Bhagiyalakshmi *et al.*, 2010).

The existing methods available for CO₂ sequestration include absorption by physical and chemical wet scrubbing, adsorption by solids using pressure and temperature swing modes, cryogenic distillation, separation of CO₂ using selective membranes and mineralization processes. However, each of these systems has its own limitations that impede its technical or economic viability in CO₂ post combustion capture systems (Ram Reddy *et al.*, 2006). Treatment using amine absorption is a widely commercialized technology for carbon dioxide removal. However, the capital and operating costs tend to be high as the carbon dioxide concentration increases. Furthermore, the captured and sequestered CO₂ offers benefits in plants for the utilization of CO₂ as feedstock in dry methane reforming, carbon gasification and other novel oxidation processes (Ding and Alpay, 2001). Carbon dioxide capture at elevated temperatures and pressures as well as at

atmospheric temperature and pressure from natural gas and flue gas effluents has attracted the attention of researchers to design potential adsorbents (Bhagiyalakshmi *et al.*, 2010).

Hydrotalcites have become an interesting class of inorganic compounds and in particular, have desirable properties as CO₂ adsorbents in post combustion capture applications (Reddy *et al.*, 2006). Hydrotalcite materials could well meet the requirements at high temperatures using pressure swing adsorption (PSA) and temperature swing adsorption (TSA) and such compounds are one of the most promising adsorbents for the sorption enhanced reaction processes for hydrogen production as well (Yong *et al.*, 2002). PSA has the disadvantage of being energy intensive and expensive.

Membranes provide an attractive alternative to PSA. The membrane process is a viable energy saving alternative for carbon dioxide gas separation since it does not require any phase transformation (Xiao *et al.*, 2009). It is simple and relatively easy to operate and control, compact and easy to scale up. Membranes with good chemical and thermal stability and high carbon dioxide selectivity/permeability make membranes beneficial and ideal for carbon dioxide separation (Noble and Stern, 1995). Polymeric membranes such as cellulose acetate, polycarbonate and polysulfone (Funk and Li, 1989) have been widely used in various industrial separation applications. However, these membranes could not withstand an environments requiring chemical and thermal endurance. An alternative and more promising candidate with excellent thermal and chemical stabilities for carbon dioxide separation is inorganic (ceramic) membrane (Hsieh *et al.*, 1996) such as

hydrotalcite. The methods for the separation of CO₂ are outlined in detail in the following section.

1.2 Methods of separation for carbon dioxide

As mentioned previously, there are many methods employed for the separation of CO₂ such as adsorption by solids, membrane separation, absorption by physical and chemical wet scrubbing, cryogenic distillation and mineralization processes.

1.2.1 Separation of CO₂ by adsorption onto hydrotalcite

Adsorption processes have been suggested as an alternative traditional separation processes such as distillation and absorption. Gaseous species are adsorbed preferentially on solid sorbents (Ko *et al.*, 2003). Adsorption involves the enrichment of one or more components in an interfacial layer between two bulk phases which are gas and solid. The adsorption mechanisms are generally governed by physical and chemical interactions that lead to physical adsorption (physisorption) and chemical adsorption (chemisorption). Physisorption is dependent on the same intermolecular attractive and repulsive forces which are responsible for the condensation of vapors whereas chemisorption is governed by the chemical bond formation between the adsorbed molecules and the surface of the solid (Kamarudin *et al.*, 2004).

Hydrotalcite possesses the capability to separate carbon dioxide by means of physisorption and chemisorption because of its appreciable mesopores areas which results in a higher exposed surface area and hence a high capacity of adsorption and

the stable interdispersion of the active species with high reproducibility (Albertazzi *et al.*, 2007, Abello and Perez-Ramirez, 2006) for adsorption of carbon dioxide. Besides that, hydrotalcite can also easily form mixed oxides. Due to the homogenous interdispersion of the constituting elements in the hydrotalcite matrix, the mixed oxides formed upon the thermal decomposition of anionic clays possess unique properties as outlined in the next section (Serwicka and Bahranowski 2004).

Hydrotalcite has long been known as one of the naturally occurring minerals. However, the first synthesized hydrotalcites were obtained in 1942 when Feitknecht mixed solutions of metal salts with the hydroxides of alkali metals (Vaccari, 1999, Yang *et al.*, 2007). Hydrotalcite is of the same regular octahedron as brucite ($\text{Mg}(\text{OH})_2$) with some Mg^{2+} replaced by Al^{3+} in which each metal cation, Mg^{2+} or Al^{3+} , is located at the center of the octahedron with hydroxyls. The partial substitution of Mg^{2+} with cations of higher charges render the layers positive and the excess charge is compensated by the presence of anions such as CO_3^{2-} , NO_3^- , Cl^- and SO_4^{2-} (Serwicka and Bahranowski, 2004). The comparison between the brucite and the hydrotalcite structures is shown in Figure 1.1.

In natural hydrotalcite mineral, the Al/Mg molar ratio is 1:3 ($x = 0.25$) where x is the Al/Mg mole fraction. However, other ratios can be obtained by artificial synthesis. It was reported that the hydrotalcite like phase could be formed in the range of a ratio (x) increased from 0.1 to 0.4. Relatively pure hydrotalcite phase might be obtained only within the range of 0.2 to 0.33 (Yang *et al.*, 2007).

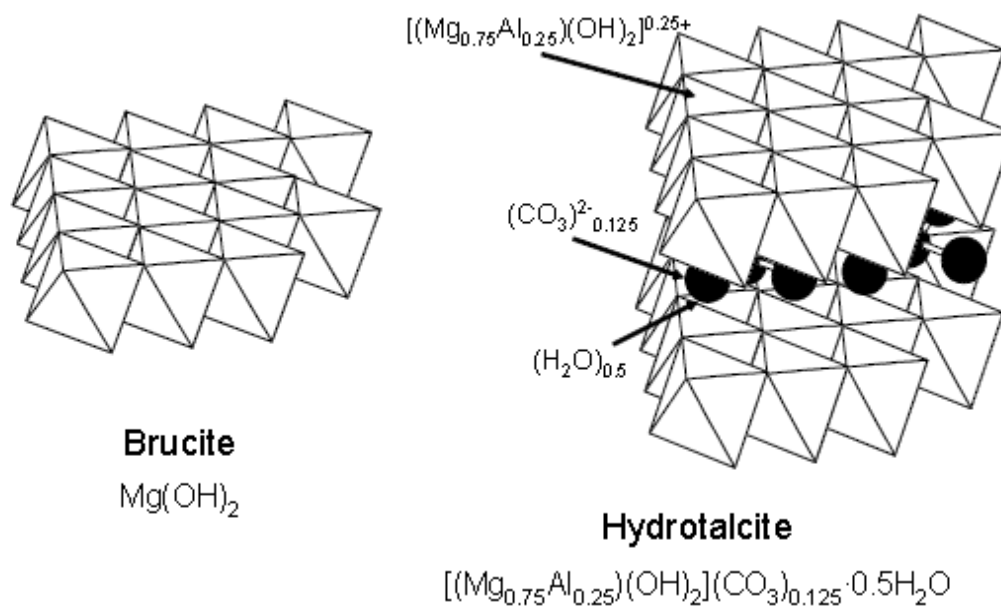


Figure 1.1: Comparison between the brucite and the hydrotalcite structures (Serwicka and Bahranowski, 2004).

Materials such as hydrotalcites or hydrotalcites modified with basic metal oxides has been considered as excellent adsorbents as well as membrane materials because of their higher carbon dioxide selectivity, adsorption capacity and selective separation at elevated temperatures as well as adequate adsorption/ desorption kinetics for carbon dioxide at operating conditions (Yong *et al.*, 2002). Stable adsorption capacity of carbon dioxide after repeated adsorption/ desorption cycles and adequate mechanical strength of adsorbent particles after cyclic exposure to high pressure streams are some other advantages of hydrotalcites.

Hydrotalcite derived mixed oxides are well known for their potential application as ion exchangers, adsorbents, catalysts and catalyst supports, filters, decolorizing agents, industrial adsorbents, polymer stabilizers, optical hosts and rheological modifiers because of their high surface area, high abrasion resistance,

high metal dispersion, high thermal stability and basic surface properties (Suarez *et al.*, 2007, Das *et al.*, 2006, Li *et al.*, 2006, Jiratova *et al.*, 2002). The applications of these materials as ionic exchangers or catalysts depend on the nature of the cations existing in the structure and on the nature of the interlayer anion (Lopez *et al.*, 1996, Suarez *et al.*, 2007). Another advantage when using hydrotalcites as precursors is that their composition can be easily modified by replacing the lamellar structure and the species located in the interlayer (Albertazzi *et al.*, 2007).

These materials have been used as adsorbents for several applications and their use in carbon dioxide adsorption at high temperatures was reported recently. This application is very important for the purification of natural gas, the possibility of CO₂ emission control in the combustion of fossil fuels and for a new steam reforming process (Othman *et al.*, 2006).

1.2.2 Separation of CO₂ by membranes of hydrotalcite

The membrane based separation of CO₂ from gas streams is an important operation applied in natural gas purification, CO₂ capture from emissions of coal fired power plants and in metabolic CO₂ removal from space life supporting systems (Xomeritakis *et al.*, 2005). The membrane separation of gas mixtures can be regarded as a simple and energy conservative with less energy consumption than in the conventional separation processes when compared with the pressure swing adsorption or liquefaction by compression and cooling (Asaeda and Yamasaki, 2001).

Two main classes of membranes which can be distinguished are dense and porous membranes. Dense membranes are made of metals, hybrid organic-inorganic or mixed conductive oxides whereas porous membranes can be an inherent feature of crystalline structures, such as zeolites, clay minerals and hydrotalcites, or be obtained by packing and consolidation of small particles (Cot *et al.*, 2000).

Porous membranes are classified into two main groups; porous and non-porous membranes. The pore diameters of macropore membranes exceed 50nm, mesopore membranes are between 2nm and 50nm and micropore membranes are less than 2nm. Transport occurs through the pores in the porous membranes rather than the dense matrix and ideal gas separation membranes possess high flux and high selectivity (Ahmad and Mustafa, 2007).

Hydrotalcite membrane which are inorganic (ceramic) membranes have been found to be promising for carbon dioxide removal and are suitable for high temperature separation processes (Conesa *et al.*, 1999, Cuffe *et al.*, 2006, Agoudjil *et al.*, 2008). They can be described as asymmetric porous materials formed by a macroporous support with successive thin layers deposited on it. The support provides mechanical resistance to the medium (Cot *et al.*, 2000). They preserve high thermal, mechanical and chemical stability, long life and good defouling properties in applications other than polymeric membranes and they have catalytic properties (Chen *et al.*, 2001, Lee *et al.*, 2006).

Hydrotalcite membranes have the potential of being used in gas separation, enrichment, and adsorptions and in filtration processes in conditions where organic

polymer membranes cannot be used. Some inorganic membranes also offer considerable promise in catalytic membrane reactor applications due to their high thermal, chemical and mechanical stability at elevated temperatures and chemically reactive environments (Othman *et al.*, 2006, Lee *et al.*, 2006).

Thus, membranes are attractive for the purification of natural gas with higher fluxes. In many cases, it is highly desirable to separate carbon dioxide from natural gas at a high temperature of approximately 400°C without cooling the gas to room temperature or even lower temperatures. This is because carbon dioxide separation at high temperature could produce concentrated and warm carbon dioxide which can be subsequently used directly as a feedstock for the chemical synthesis of fuels. This application requires a membrane or adsorbent that is selectively permeable to or adsorptive for carbon dioxide at high temperatures for which inorganic membranes such as hydrotalcite membranes could be a good candidate. The following section presents information on the hydrotalcite membranes which are generally produced using sol gel technique (Cot *et al.*, 2000, Asaeda and Yamasaki, 2001, Ahmad *et al.*, 2005, Xomeritakis *et al.*, 2005, Othman and Kim, 2008).

Hydrotalcite membranes are inorganic membranes prepared using sol gel technology. Interest in sol gel technology has increased rapidly in recent years because of the impact on the development of high-tech materials with a wide spectrum of applications which include adsorbents, catalysts, membranes and thin film optical and electronic devices. The sol gel method has been shown to produce hydrotalcite membranes with modified textural properties of hydrotalcite and their calcination products (Payro and Llacuna, 2006, Aramendia *et al.*, 2002).

Sol gel is a process which converts a colloidal or polymeric solution (sol) to a gelatinous substance (gel). It involves hydrolysis and condensation reactions of alkoxides or salts dissolved in water or organic solvents. In most of the sol gel processes, a stable sol is first prepared as an organometallic oxide precursor, followed by the addition, if necessary, of some viscosity modifiers and binders. The thickened sol is then deposited as a layer on porous support by dip or spin coating. This is followed by gelation of the layer upon drying to form a gel which is the precursor to a ceramic membrane prior to controlled calcinations.

The sol gel method is reported to be able to control pore size, surface area and the uniformity of particle dispersion in a solution leading to an effective hydrotalcite membrane (Othman *et al.*, 2006). This method exhibits larger specific areas than those obtained using a conventional co-precipitation procedure (Tichit *et al.*, 2005). This method has the ability to precisely control stoichiometry, producing multi component materials that were not available previously and having the ability to produce high purity materials for electronics and optics without much investment in equipment. Nevertheless, this method leads to a waste of solvent, large volume shrinkage during drying and high precursor cost. The sol gel method has generated considerable commercial interest because of the versatility of the process in producing multi component homogenous compositions with ease and cost effectiveness (Sangeeta and LaGraff, 2005).

1.2.3 Other methods

Other methods available for CO₂ sequestration include absorption by physical and chemical wet scrubbing, cryogenic distillation, and mineralization processes

besides adsorption by solids using pressure and temperature swing modes and CO₂ selective membranes as mentioned before.

Most adsorbents for CO₂ at high temperatures are composed of alkali metal oxides that utilize their basic properties for adsorbing CO₂. Alkali metal oxides such as calcium oxides, magnesium oxides and aluminium oxides are basic and suitable for adsorbing CO₂ at high temperatures (Yang and Kim, 2006). Also hydroxides of calcium and sodium too are used in absorption of CO₂. Ionic liquids such as amine have been applied commercially in the purification of gases for CO₂ absorption. They can reduce the use of hazardous and polluting organic solvents due to their unique characteristics (Keskin *et al.*, 2007). Although amine treatment is a commercialized technology in which the hydrocarbon loss is almost negligible, the capital and operating cost increase rapidly as the concentration of carbon dioxide in the feed gas increases (Datta and Sen, 2006).

Chemical absorption has been used successfully for low pressure gas streams but the large solvent regeneration costs associated with the process hamper its application to higher CO₂ contents. The degree of absorption is limited by the fixed stoichiometry of the chemical reaction. As a consequence, the use of this process for CO₂ gas streams will lead to high solvent circulation flow rates and high energy requirements. The amount of CO₂ absorbed by the solvent is determined by the vapor liquid equilibrium of the mixture which is governed by the pressure and temperature. At high CO₂ partial pressure, the CO₂ loading capacity of the solvent is higher for a physical solvent than for a chemical solvent.

Cryogenic distillation is used for the removal of nitrogen from natural gas and it is highly energy intensive. The separation energy for cryogenic distillation in the production of natural gas and ethylene is reported to be high (www.processregister.com). However, this method is only viable for CO₂ concentration of more than 90 volume percent which is outside the range of CO₂ concentrations in flue gas streams (Reynolds *et al.*, 2005) and natural gas.

Mineralization processes such as mineral carbonation which sequesters CO₂ as a mineral carbonate has recently attracted much interest because of its ability to remove CO₂ with a spontaneous and exothermic reaction. Hence it has a great potential to become economically feasible. In addition, mineral carbonation is also expected to offer an environmentally safe and permanent CO₂ disposal method (Kodama *et al.*, 2008).

However, each of these systems has their own limitations that impede their technical or economic viability in CO₂ post combustion capture systems (Ram Reddy *et al.*, 2006). Among these, physical absorption using amine solvents is the only technology that is currently deployed commercially for CO₂ capture. However, there is a significant energy penalty associated with this technology because of the heat required to regenerate the solvent (Hutson *et al.*, 2004).

The capture of CO₂ has become an important research issue of global proportions as more international attention is focused on global warming. Therefore, among the various sequestration technologies such as CO₂ capture by pressure swing adsorption, PSA and temperature swing adsorption, TSA is a promising option for

separating CO₂ considering its relatively low operating and capital costs, eco-compatibility and flexibility (Zhang *et al.*, 2008, Tagliabue *et al.*, 2009).

1.2.4 Gas diffusion

Delgado *et al.* (2007) observed that CO₂ diffuses into adsorbents faster than methane (CH₄). It is well known that surface diffusion can contribute significantly to the total transport in a porous medium. This contribution is more pronounced for small pore diameters at lower pressures, that is, in the region where Knudsen diffusion prevails (Argonul *et al.*, 2007). Also, pore diffusion governs the internal transfer of organic substances of solid particles. In this case, the adsorbate diffuses through the gas filled pores in its original form and by solid phase diffusion in which case the adsorbate is transferred in its adsorbed form usually via surface diffusion along the pore walls (Gaid *et al.*, 1994).

Diffusion is usually described by two diffusion coefficients; one for transport in the micropores and another for transport in the macropores. In principle, mass transport in porous particles involves four basic mechanisms: bulk or free molecular diffusion, Knudsen diffusion, surface diffusion and viscous diffusion (Mugge *et al.*, 2001, Rudzinski and Plazinski, 2007). All the mechanisms may affect distinguishing the kinetics which is governed by internal diffusion and in which surface reaction controls the rate of sorption in the adsorption system (Rudzinski and Plazinski, 2007). These diffusion models will be further discussed in Section 2.3.

1.3 Problem Statement

Natural gas is composed mainly of 85% to 95% methane. Approximately 5% of CO₂, nitrogen and small amounts of higher molecular weight hydrocarbons such as ethane, propane and butane (Datta and Sen, 2006, Esteves *et al.*, 2008) from the balance.

The calorific value of natural gas is lowered by the presence of CO₂. Also CO₂ leads to higher volumes per unit heating value that requires higher handling of the volume of natural gas in its applications. Removal of CO₂ is also required because of the existence of gas that can lead to corrosion in the transportation of pipelines. Hence, the CO₂ content in natural gas needs to be lowered to meet the required pipeline specification of 2% to 5% carbon dioxide (Datta and Sen, 2006).

Based on the previous discussions, it is found that hydrotalcite is a good choice for the removal of CO₂ from natural gas. However, powder handling becomes difficult in processes related to hydrotalcites. In addition, membranes prepared using the sol gel method is often found to have difficulties in large scale applications.

Research carried out so far include the study of CO₂ separation using hydrotalcite in powder form and membrane form (Othman *et al.*, 2006, Ye Lwin and Abdullah, 2009, Kim *et al.*, 2009). These studies usually involved equilibrium capacities and transport of CO₂ through sol gel hydrotalcite membranes (Mayorga *et al.*, 2001). Very little research is available in order to evaluate the rates of separation of CO₂ via these processes (Ye Lwin Abdullah, 2009).

In commercial application, the viability of the process generally depends on the extents of the rates of separation. On the other hand, handling of powders of hydrotalcite in commercial applications is cumbersome. Pelletized hydrotalcite could be useful in such situations. The pellets should be mechanically strong in order to sustain stringent environments of reactions such as in fluidized beds. For this purpose, pellets coated with hydrotalcite could be a good selection because of the ceramic nature of the hydrotalcite coats and the selective separation behavior of the sol gel coats. This research is aimed at studying the rates of adsorption of CO₂ on powders, coated and uncoated pellets of hydrotalcite.

1.4 Objectives

The present research aims to achieve the following specific objectives which are:

1. To study the properties adsorption of synthetic and commercial hydrotalcite using Brunauer Emmett and Tellet (BET) analyzer and X-ray Diffraction (XRD) analyzer in order to obtain a suitable test material for experimentation.
2. To evaluate the rate of adsorption of carbon dioxide on selected hydrotalcite samples in powder form and on pelletized hydrotalcite based on Design of Experiments (DoE) analysis with temperatures of reaction, diameter of hydrotalcite pellets, and number of coatings of sol gel hydrotalcite as parameters.
3. To investigate the criteria which given the adsorption rate of CO₂ in hydrotalcite using existing models and a developed model.

1.5 Scope of Study

In the first part of this study, an experimental rig consisting of a batch reactor was fabricated for carrying out adsorption of carbon dioxide on hydrotalcite powder and hydrotalcite pellets. The batch reactor could withstand high temperatures up to 1000°C with a variable temperature controller.

Synthetic hydrotalcite was prepared using the optimized condition of the coprecipitation method as reported from a previous study. Synthetic hydrotalcite prepared and commercial hydrotalcite (Tomita-AD 500) were compared using X-ray Diffraction (XRD) and Brunauer Emmett and Teller (BET) method in order to identify a suitable sample material for testing.

Commercial hydrotalcite was thereafter selected and used for further studies for the rates of adsorption of CO₂ on hydrotalcite materials. The hydrotalcite powders were pressed into three pellet sizes which are 8mm, 15mm and 20mm in diameter of 0.5mm in thickness. Later, the pellets were coated with hydrotalcite sol prepared using the sol gel method to form a thin layer on the pellet surface. These pellets were used as the pellet samples for experiments.

5% CO₂ in nitrogen was used in order to investigate the rates of adsorption. 5% CO₂ concentration was particularly used to simulate the concentration of CO₂ in the natural gas as mentioned in Section 1.1. Several parameters, which are temperature of reaction, diameter of hydrotalcite pellets and number of sol coatings, were studied using the Design of Experiment (DoE) method. Finally, the evaluated results were then analyzed and compared using several mathematical models.

1.6 Organization of the Thesis

There are five chapters in the thesis and each chapter provides important information of the thesis. In the first chapter, a brief introduction about the need for carbon dioxide separation from gases, the types of separation technologies used today and the reasons for selection of hydrotalcite material for the removal of carbon dioxide in this study are given. In the problem statement, several problems required to be solved are listed. The needs for hydrotalcite in pellet form and in coated form with hydrotalcite sol are explained briefly. Thereafter, objectives are outlined which guided this study.

Chapter two presents the literature review consisting of the introduction of hydrotalcite in detail. This is followed by the outlining separation technologies used to remove carbon dioxide using hydrotalcite materials, which are adsorption and the membrane treatment. Several theoretical studies on gas solid adsorption are also discussed.

Chapter three covers the detailed description of the materials, the equipment and the experimental rig used, the preliminary studies on hydrotalcite materials, the details of experiments carried out and finally, the statistical analysis and mathematical modeling.

Chapter four presents the experimental results and discussion thereof. It is divided into four sections. The first section covers the results and the discussion for the preliminary studies of the hydrotalcite material. Statistical analysis using the Design of Experiment (DoE) is covered in the second section. The third section

explains the results and discussion on the variation of the adsorption of hydrotalcite in the batch process with temperature of reaction, diameter of hydrotalcite pellets and the number of coatings. In the final section, the comparison of the results based on the experimental data and the mathematical models are discussed and the probable mechanism which given the rates of adsorption identified.

Finally, Chapter five summarizes the conclusions obtained in the present research. Some recommendations are also given in order to improve the research work as well as the future direction of the current study.

CHAPTER TWO

LITERATURE REVIEW

2.1 Hydrotalcite

2.1.1 General description

Hydrotalcites are a new large family of layered inorganic materials with positive structural charges with the general formula of $[M_{1-x}^{2+}M_x^{3+}(OH)_2]^{x-}[A_{x/n}^{n-}]_mH_2O$ where M^{2+} (Mg^{2+} , Zn^{2+} , Ni^{2+} etc) and M^{3+} (Al^{3+} , Cr^{3+} etc) are divalent and trivalent metal cations respectively. The layers are positively charged as M^{3+} cations substitute M^{2+} cations. This charge is balanced by A anions with charge n^- (Davila *et al.*, 2008). A^{n-} is the charge compensating the anion or gallery anion such as CO_3^{2-} , Cl^- and SO_4^{2-} , m is the number of moles of co-intercalated water per formula weight of the compound, and x is the number of moles of M^{3+} per formula weight of the compound and is normally between 0.17 and 0.33 [Hutson *et al.*, 2004]. The general formula of hydrotalcite is $Mg_6Al_2(OH)_{16}CO_3 \cdot 4H_2O$ (Lopez, *et al.*, 1997).

Hydrotalcite, also known as double layered hydroxides (LDH), is found as a natural layered mineral or so-called anionic clay, constituting of a class of lamellar ionic compound. These materials have received much attention because of their wide range of applications as catalysts, precursors and adsorbents (Ram Reddy *et al.*, 2006). Hydrotalcite contains a positively charged (cations) hydroxide layer or brucite sheet and charge-balancing anions which are carbonates in the interlamellar space besides water molecules as shown in Figures 2.1 and 2.2.

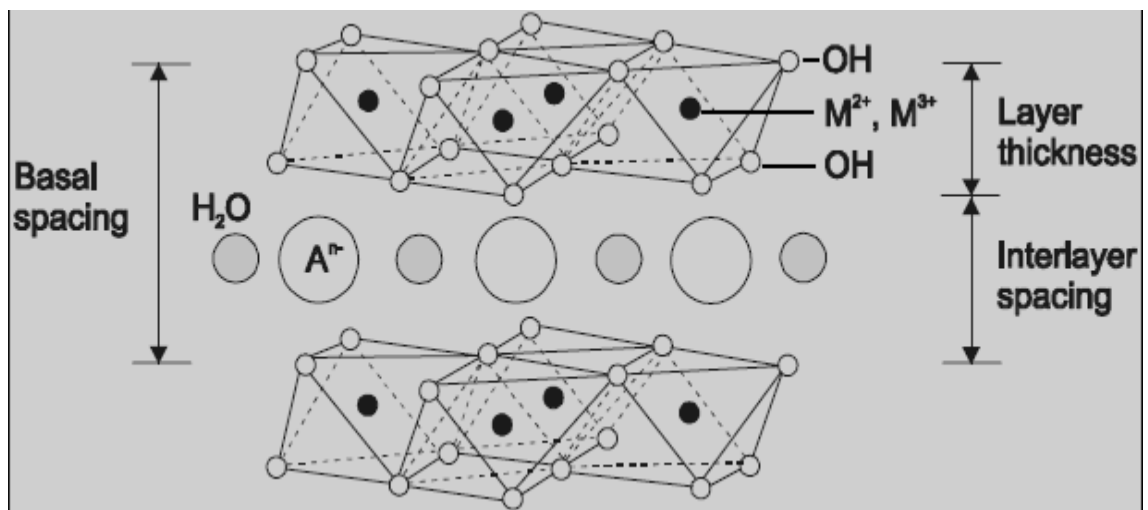


Figure 2.1: 3-D structure model for hydrotalcite (Tsunashima and Toshiyuki, 1999).

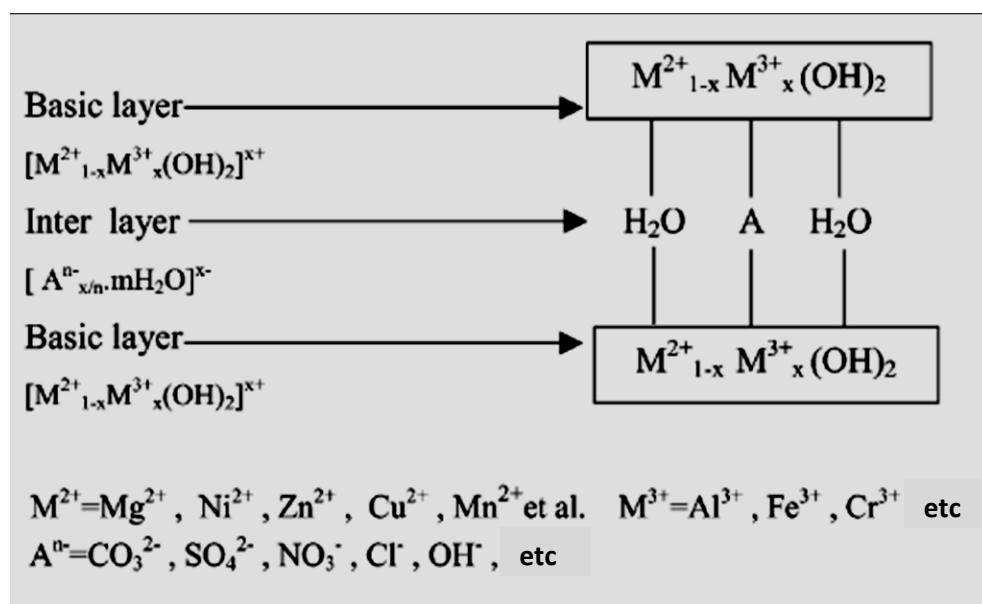


Figure 2.2: 2-D structure models for hydrotalcite (Yong and Rodrigues, 2002).

The positive charges in the layers have also been termed as permanent positive charges and they are compensated by the hydrated anions between the stacked sheets. In recent years, interest has grown in the preparation, characterization